NUMERICAL FLOW INVESTIGATION OF AN ANNULAR S-SHAPED DUCT

Jinhan Kim*, Chang Ho Choi*, Jungu Noh*, Daesung Lee*
***Korea Aerospace Research Institute**
P.O.BOX 113, Yusung, Taejun, Korea

Keywords: *Numerical flow analysis, S-shaped duct, compressor*

Abstract

This paper is concerned with the numerical flow analysis of an S-shaped duct for the inter-channel between compressor spools. For the compactness and lightweight of an engine, the length of the S-shaped duct is desired to be minimized. Shortening the S-shaped duct, however, flow separation is likely to occur.

Numerical investigation using a three-dimensional Navier-Stokes flow solver has been performed to determine the availability of the minimization of an S-shaped duct adopting available experimental data as the inlet flow condition of the S-shaped duct.

1 Introduction

Since each compressor spool has a different mean radius, the flow within the connecting ducts must undertake a corresponding change in radius. Thus, annular S-shaped ducts are widely adopted on multi-spool gas turbine engines. To minimize engine weight, however, this change in radius must be achieved within the shortest possible length that is consistent with the avoidance of flow separation.

Studies to clarify the flow behavior on S-shaped duct are introduced by Britchford et. al. [1,2] comparing the experimental data and CFD results. From these studies, it is shown that the flow within the duct is significantly influenced by the effects of streamwise pressure gradients and flow curvature [2]. Bailey and Carrotte [3] investigated on the effect of inlet swirl on S-Shaped duct which may be a one of the important matters in S-Shaped duct design in engines. To simulate further practical configuration, a strut was employed and the performance of S-Shaped duct was provided by Bailey et. al. [4]. Further steep S-Shaped duct with tangentially leant OGV are studied by Britchford et. al. [5]. The leant OGV is considered to assist the flow radially inward.

Previous studies provided the detail flow structures in S-Shaped ducts for various flow conditions. It is considered that the S-Shaped duct introduced by Britchford et. al. [1] seems to have enough margins from separation limit. For the compact design of S-shaped duct, limits of design parameters better be investigated.

This paper is an initial attempt to find the limit in reducing the S-Shaped duct length and radius.

2 Configuration of the S-shaped Duct

Experimental studies on the present S-shaped duct shown in Fig. 1 and 2 were conducted at Loughborough university [1,2]. Rows of compressor rotor and OGV (outlet guide vane) are located upstream of the S-shaped duct. Figure 3 shows the locations of measurement planes where A1 indicates inlet and A8 outlet of the S-shaped duct. Detail description of the experimental facility and test conditions are given by Britchford et al. [1,2].

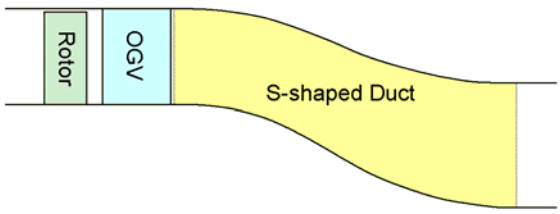

Fig. 1 Configuration of the S-shaped Duct

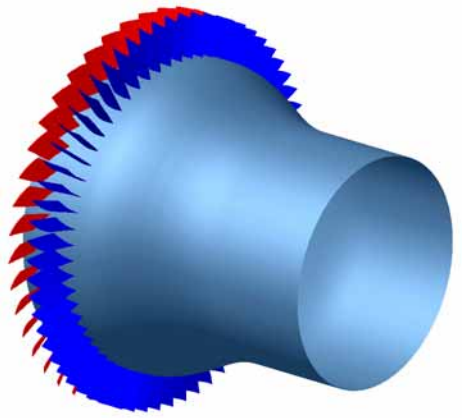

Fig. 2 Three-Dimensional View of the S-shaped Duct

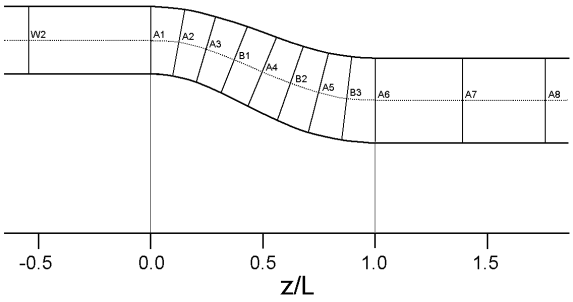

Fig. 3 Locations of the Traverse Plane

3 Computational Model

In the present study, a commercial 3-D RANS (Reynolds Averaged Navier-Stokes) method is adopted [6]. The method employs an explicit Runge-Kutta scheme and second-order accurate central-difference with added artificial dissipations for the integration in time and space, respectively.

Britchford et al. [1,2] compared two turbulence models(i.e., k-ε and Reynolds stress models) reporting that the mean velocity profile and shear stress are predicted better by the latter. They also indicate that the Reynolds stress model can predict much better than the k-ε model for the critical cases when likely to be close to separation. However, in the present study, the k-ε model is used as a turbulence closure to save the computational effort aiming at the process as a part of developing design procedure.

The Yang-Shih k-ε turbulence model is used to simulate turbulence effects. To accelerate the convergence of the solution, locally varying time-step, implicit residual smoothing and multigrid schemes are adopted to the governing equations.

At the beginning stage of this study, computations including the rotor blades with OGV were carried out employing a mixing-plane method in between rotor and OGV for a fast convergence instead of a time consuming unsteady calculation. Comparing the numerical results with experimental data, it turned out that the mixing plane attenuated the wake flow of the rotor blades. Thus, the inlet boundary flow conditions of the OGV and S-shaped duct showed differently from the experimental data. It is known that the mixing-plane method can predict the overall performance fairly well with less computational efforts. The detail flow structure, such as boundary layers, wake flows etc., however, can not be predicted properly [7]. Thus, estimation of S-shaped duct limit using mixing plane method seems not acceptable.

In the present study, the rotor blades with OGV are excluded in the calculations introducing the available measured data as the inlet flow condition of the S-shaped duct.

In order to predict the flow in the S-shaped duct accurately, it is important to ensure that the inlet boundary conditions match with the measurements. Unfortunately, ε values are not available. In the present study, a conventional assumption that turbulent viscosity is 50 times greater than the molecular one is applied for the ε values at the inlet [6]. Static pressures are assigned at the outlet of the duct and periodic boundary conditions are set to solve one blade passage only.

4 Results and discussions

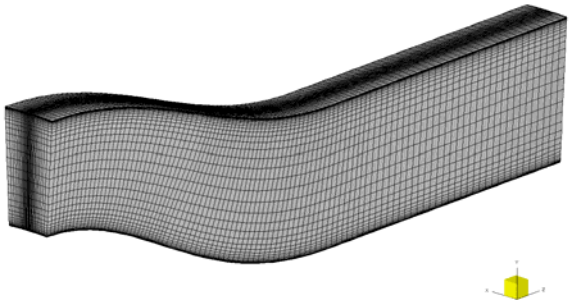

Fig. 4 Computational Grid (65X37X145)

In order to verify the current CFD method, calculations are performed on the S-shaped duct only for which experimental data are reported by Britchford et al. [1]. Figure 4 shows the computational mesh with cells clustered to simulate the accurate wake flow arising from the upstream OGV.

Figure 5 shows pressure coefficient variations along axial direction where a strong adverse pressure gradient exists on the inner wall (hub). On the outer wall (shroud), also a strong zone exists at the down stream region while a mild adverse pressure gradient showed at entry region. It is considered that the development of the boundary layer is significantly affected by the static pressure distribution near the wall.

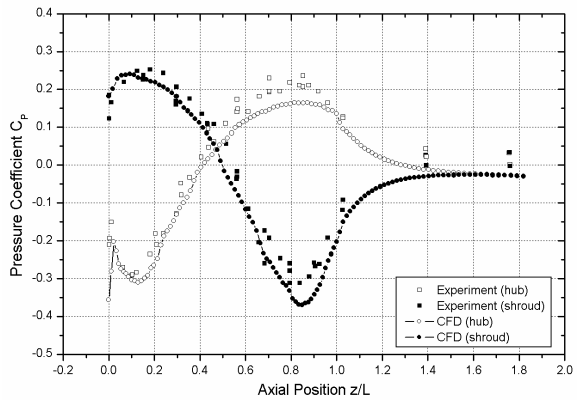

Fig. 5 Measured and Predicted Axial Variation of the Pressure Coefficient

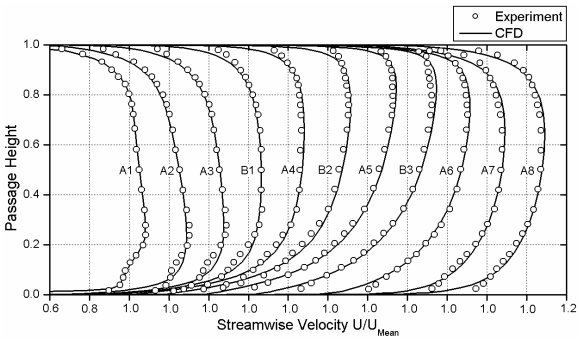

Fig. 6 Measured and Predicted Streamwise Velocity Profiles

Figure 6 presents predicted velocity profiles in comparison with the experimental data. The CFD results show under estimated in velocity near the wall due to the inaccuracy of the turbulence model. But, the overall agreement with the measurement seems in fair agreement. The flow near the inner wall is accelerated at first, but strong deceleration and thickening of the boundary layer followed due to the adverse pressure gradient region downstream. In the mean time, the boundary layer at the outer wall shows an initial deceleration and then acceleration occurs. But, boundary-layer thickening near the exit follows due to the adverse gradient.

Figure 7 shows contour plots of the velocity components at three traverse planes. The measured data which is used as the inlet boundary conditions of the calculation at the plane A1 is shown on Fig. 7(a). At all planes, the effects of the wake flow downstream of the OGV are apparent. Along the S-shaped duct, thickening of the boundary layer at the inner wall is shown. Radially inward flow (negative V_r) also can be observed. The computation predicts thicker boundary layer at the inner wall and stronger radially inward flows compared to the measurements. However, the predicted results are comparable with the trend of the experimental ones and fair enough to understand the flow behavior.

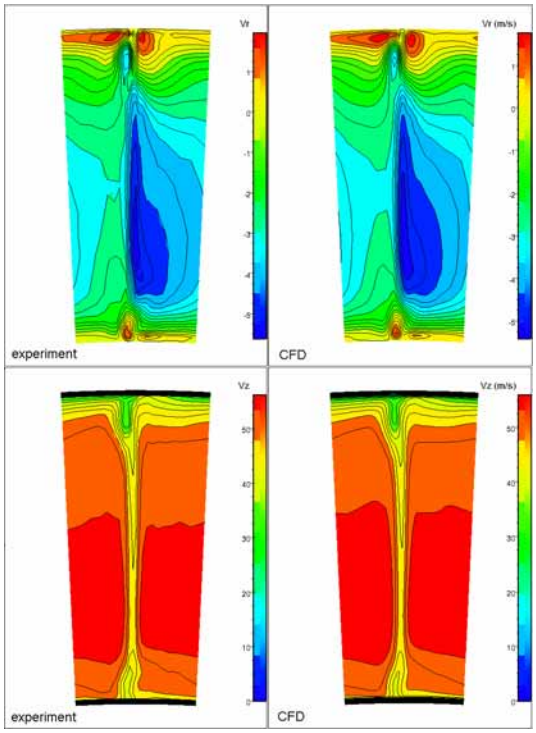

(a) traverse plane A1

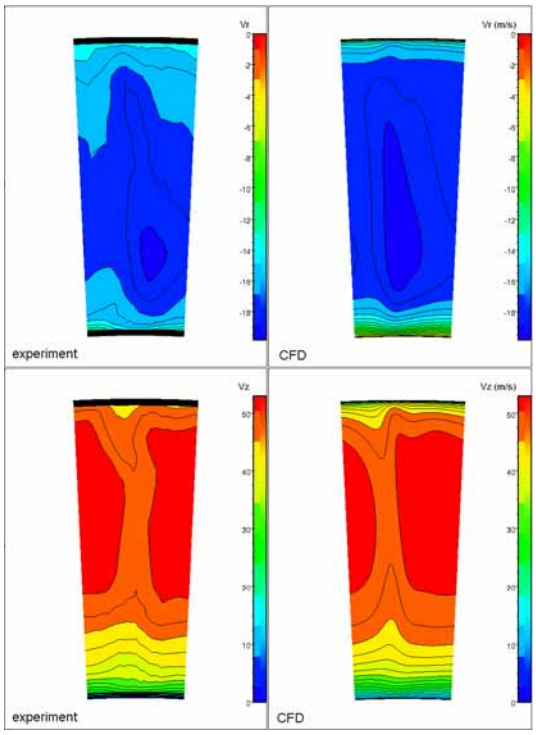

(b) traverse plane A4

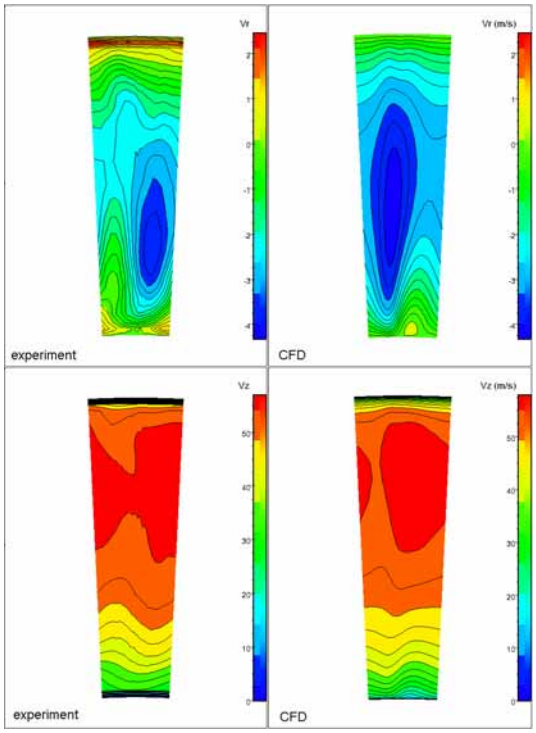

(c) traverse plane A6

Fig. 7 Contours of the Velocity Components

Based on these results, it is considered that the current computational scheme provides conservative values in determining the compactness of S-shaped duct.

Further efforts concerning to the compact design of the S-shaped duct are followed subsequently. The length and the radius of the S-shaped duct are reduced until flow separation is occurred. In the present study, the effects of the length and the radius of the duct are investigated separately keeping the passage areas constant along the mean line to maintain the geometric similarity. Figure 8 shows the limit length and radius before flow separations start to evolve. It is concluded that the axial length can possibly be reduced up to 76% of the original length and the radius up to 83% as well.

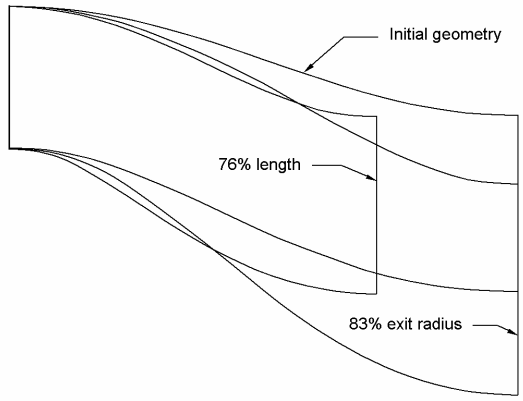

Fig. 8 Geometry Modification

Figure 9 shows resulting velocity profiles and wall pressure coefficient distributions along the passage. As the length or radius is reduced, the adverse pressure gradient becomes stronger near the inlet and the boundary layer is thickened on the inner wall. And a strong adverse pressure develops at the outer wall exit where originally a mild pressure gradient is observed. The velocity profiles show that the separation regimes are near especially at the regions of B2 and A5.

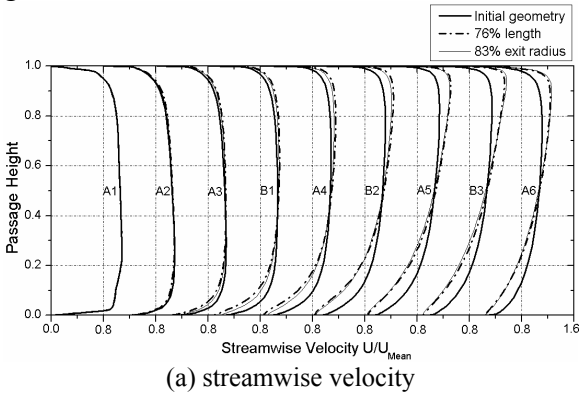

(a) streamwise velocity

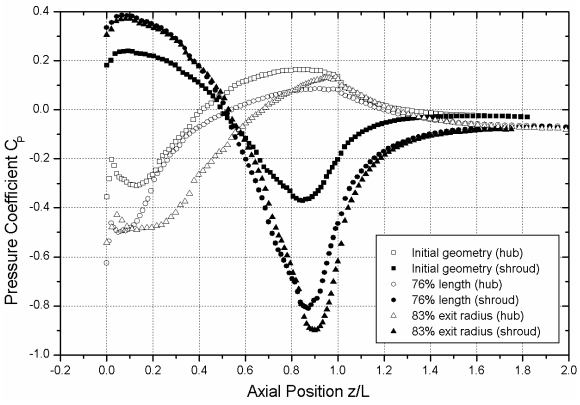

(b) pressure coefficient

Fig. 9 Velocity and Pressure Coefficient Distributions

5 Conclusions

Computational studies on the S-shaped duct are conducted. The conclusions are as follows;

(1) The CFD results when the inlet condition of S-shaped duct is adopted from the mixing plane method showed quite differently from the results obtained from the inlet condition of experimental data. Thus, estimation of S-shaped duct limit using mixing plane method seems not acceptable.

(2) The present predictions agree reasonably well with the available measurements except near wall regions which is caused from the inaccuracy of the turbulence model. Thus, it is considered that the present method can be applied as a tool for the design modification of the S-shaped ducts.

(3) It is considered that the present S-shaped duct has enough margins from separation and its limits are shown when reduced lower than 76% of the axial length and lower than 83% of the radius.

Acknowledgements

The authors would like to express their special thanks to K. Britchford and J. Carrotte for their assistance and close communications.

Reference

[1] Britchford, K.M., Manners, A.P., McGuirk, J.J. and Stevens, S.J. Measurements and Prediction of Flow in Annular S-shaped Ducts. *Proceedings of the Second International Symposium on Engineering Turbulence Modelling and Measurements*, Florence, Italy, pp 785-794, 1993.

[2] Britchford, K.M. Carrotte, J.F., Stevens, S.J. and McGuirk, J.J. The Development of the Mean Flow and Turbulent Structure in an Annular S-shaped Duct. 94-GT-457, 1994.

[3] Bailey, D.W. and Carrotte, J.F. The Influence of Inlet Swirl on the Flow within an Annular S-Shaped Duct. 96-GT-60, 1996.

[4] Bailey, D.W., Britchford, K.M., Carrotte, J.F., and Stevens, S.J. Performance Assessment of an Annular S-Shaped Duct. *Journal of Turbomachinery*, Vol. 119, pp 149-156, 1997.

[5] Britchford, K.M., Carrotte, J.F., Kim, J.H., Hield, P.M. The Effect of Operating Conditions on the Aerodynamic Performance of an Integrated OGV and S-Shaped Duct. 2001-GT-0347, 2001.

[6] Numeca Inc. Fine/Turbo Manual for Version 5.13, 2002.

[7] Choi, C.H. and Yoo, J.Y. Unsteady Blade-Row Flow Calculations Using a Low Reynolds-Number Turbulence Model. *Journal of Propulsion and Power*, Vol. 16, No. 5, pp 768-776, 2000.